

Original article

УДК 597.552.511–148.85

DOI: 10.26428/1606-9919-2022-202-305-315

EDN: AXPBZX



STRONTIUM SIGNAL LAG IN OTOLITHS OF JUVENILE
SOCKEYE SALMON (*ONCORHYNCHUS NERKA*) DURING TRANSITION
FROM THE FRESHWATER TO MARINE ENVIRONMENTS

Yu. Kuzmenko¹, B.P.V. Hunt^{1,2,3}, Yu. Egorova¹, T. Spesivy²,
S.C. Johnson⁴, E.A. Pakhomov^{1,2,3*}

¹ Department of Earth, Ocean and Atmospheric Sciences, University of British Columbia,
2207 Main Mall, Vancouver, British Columbia, Canada V6T 1Z4;

² Institute for the Oceans and Fisheries, University of British Columbia,
2202 Main Mall, Vancouver, British Columbia, Canada V6T 1Z4;

³ Hakai Institute, P.O. Box 309, Heriot Bay, BC, Canada V0P 1H0;

⁴ Fisheries and Oceans Canada, Pacific Biological Station,
3190 Hammond Bay Rd, Nanaimo, BC, V9T 6N7

Abstract. The shift in strontium (Sr) concentrations in fish otoliths is a commonly used proxy for identification of marine environment entry during diadromous migrations. However, there is still controversy about the appearance of the Sr-based sea entry mark relative to the true point of entry. In this study, the Sr signal lag was assessed in otoliths of juvenile sockeye salmon (*Oncorhynchus nerka*) under experimental conditions replicating the transition to seawater during juveniles' seaward migration. A Sr signal delay was observed to average at 8.2 (SD = 5.1) days for fish with a body length of 140–170 mm (and a weight of 30–70 g). This lag may be species-specific and should be taken into consideration when estimating marine entry timing and marine residence duration of juvenile salmon.

Keywords: Sr signal lag, LA-ICP-MS, sockeye salmon, otoliths, trace elements

For citation: Kuzmenko Yu., Hunt B.P.V., Egorova Yu., Spesivy T., Johnson S.C., Pakhomov E.A. Strontium signal lag in otoliths of juvenile sockeye salmon (*Oncorhynchus nerka*) during transition from the freshwater to marine environments, *Izv. Tikhookean. Nauchno-Issled. Inst. Rybn. Khoz. Okeanogr.*, 2022, vol. 202, no. 2, pp. 305–315. DOI: 10.26428/1606-9919-2022-202-305-315. EDN: AXPBZX.

* Kuzmenko Yulia, post-graduate student, ykuzmen@eoas.ubc.ca, ORCID 0000-0002-7939-8095; Hunt Brian P.V., assistant professor, b.hunt@oceans.ubc.ca, ORCID 0000-0003-4718-4962; Egorova Yulia, post-graduate student, yegorova@eoas.ubc.ca, ORCID 0000-0002-8712-7789; Spesivy Tymofey, laboratory technician, tim.spesivy@gmail.com; Johnson Johnson C., research scientist 2nd degree connection, Stewart.Johnson@dfo-mpo.gc.ca; Pakhomov Evgeny A., Ph.D., professor, director of institute, epakhomov@eoas.ubc.ca, ORCID 0000-0002-6145-2129.

© Kuzmenko Yu., Hunt B.P.V., Egorova Yu., Spesivy T., Johnson S.C., Pakhomov E.A., 2022

Задержка сигнала стронция в отолитах ювенильной нерки (*Oncorhynchus nerka*) во время перехода из пресной в морскую среду

Ю. Кузьменко¹, Б. Хант^{1,2,3}, Ю. Егорова¹, Т. Спесивый², С. Джонсон⁴, Е. Пахомов^{1,2,3}

¹ Департамент земных, океанических и атмосферных наук университета Британской Колумбии, 2207 Main Mall, Vancouver, British Columbia, Canada V6T 1Z4;

² Институт океана и рыболовства университета Британской Колумбии, 2202 Main Mall, Vancouver, British Columbia, Canada V6T 1Z4;

³ Хакай институт, P.O. Box 309, Heriot Bay, BC, Canada V0P 1H0;

⁴ Fisheries and Oceans Canada, Тихоокеанская биологическая станция, 3190 Hammond Bay Rd, Nanaimo, BC, V9T 6N7

Аннотация. Изменение концентраций стронция в отолитах рыб повсеместно используется как прокси диадромных миграций. Однако позиция метки стронция по отношению к точной (или истинной) точке перехода оставалась спорной. В этом исследовании была измерена задержка сигнала стронция в отолитах нерки, содержащейся в экспериментальных условиях, приближенных к условиям, в которых рыба совершает раннюю морскую миграцию. Описанная задержка сигнала стронция составила в среднем 8,2 (СД = 5,1) дня для рыб размером 140–170 мм и массой 30–70 г. Такая задержка может быть видоспецифичной и должна учитываться при расчетах перехода в морскую среду и продолжительности раннего морского периода с использованием концентрации стронция в отолитах нерки.

Ключевые слова: задержка сигнала стронция, лазерная абляция, нерка, отолиты, микроэлементы

Для цитирования: Кузьменко Ю., Хант Б., Егорова Ю., Спесивый Т., Джонсон С., Пахомов Е. Задержка сигнала стронция в отолитах ювенильной нерки (*Oncorhynchus nerka*) во время перехода из пресной в морскую среду // Изв. ТИНРО. — 2022. — Т. 202, вып. 2. — С. 305–315. DOI: 10.26428/1606-9919-2022-202-305-315. EDN: AXPBZX.

Introduction

The calcified body structures of fish are considered valuable recording structures that can be used as archives of life-history data in ecological studies. The shape, microchemistry, and microstructure of fish scales, bones, and otoliths can provide information on fish habitat use, migrations, and physiological state at a daily to yearly resolution [Campana, 1999]. Among these, otoliths, being metabolically inert and having daily growth records which makes them a highly reliable data source, are usually selected as the most useful high-resolution data archives [Campana, Thorrold, 2001]. Employment of microchemistry and microstructure of otoliths can, therefore, provide high-resolution information on diverse aspects of fish biology and environmental conditions experienced by fish.

Strontium (Sr) concentration profiles in otoliths are used increasingly to identify shifts between freshwater and marine habitats in diadromous fishes including salmon [Campana, 1999; Yokouchi et al., 2011; Stocks et al., 2014; Freshwater et al., 2015]. However, a variety of intrinsic and extrinsic factors influence incorporation of Sr and other trace elements into otoliths. This may lead to shifts in the ratio of ambient environmental to otolith elemental concentrations and complicate life history reconstruction [Campana, 1999; Bath et al., 2000; Campana et al., 2000; Elsdon et al., 2008; Kerr, Campana, 2014]. In addition to environmental concentrations, physiological factors such as metabolic rates, growth as a response to feeding conditions, and reproduction also significantly affect elemental incorporation into otoliths in several fish species [Villiers et al., 1995; Yokouchi et al., 2011; Nelson, Powers, 2019]. To address the complexity of otolith signal formations, it has been proposed to use a combination of chemical and microstructural markers to identify the marine entry point [Freshwater et al., 2015]. However, even this may not be a reliable approach due to the appearance of multiple check marks in wild fish otoliths with long saltwater or freshwater residence time [Campana, 1999]. Moreover, earlier attempts to validate microstructural marks relative to

Sr signals yielded contradictory results, where the Sr signal of marine entry appeared earlier than the microstructural check mark, which was attributed to the physiological changes in fish prior to leaving freshwater habitat [Zhang, Beamish, 2000; Freshwater et al., 2015].

For Pacific salmon, the transition between saltwater and freshwater habitats is considered a critical time [Beamish et al., 2004; Welch et al., 2013], and the subsequent early marine life-history phase is hypothesised to be a key determinant of recruitment success [Irvine, Akenhead, 2013; nparc.org/science-plan/]. Understanding juvenile salmon experience and survival during this life-history phase requires well-resolved, accurate information on the timing of entry, size at entry, migration, and early marine growth rates [Henderson, Cass, 1991; Koenings et al., 1993]. Although both otolith microstructure [Zhang, Beamish, 2000] and microchemistry [Walther, Limburg, 2012; Nelson, Powers, 2019] have been used for this purpose, questions as to time lags remain unresolved for the latter. Limited studies suggested that the Sr signal delay may be as little as 2–3 days in salmon or up to 10 days in eel [Miller, 2011; Yokouchi et al., 2011]. For salmon, previous studies reported contradictory results: e.g., Miller [2011] found a 2–3-day delay in the Sr signal appearance in Chinook juveniles (*Oncorhynchus tshawytscha*) relative to the true sea entry point, while Freshwater et al. [2015] found that the Sr signal appeared several days before the visual microstructure check mark and the true saltwater entrance point. This study aimed mainly to measure the Sr signal appearance under controlled experimental conditions and identify the relationship of the Sr signal with the true sea entry point in juvenile sockeye salmon (*Oncorhynchus nerka*) using highly (nearly daily) resolved data obtained by the Laser Ablation Inductively Coupled Plasma Mass Spectrometry (LA-ICP-MS).

Materials and methods

Experimental setup. We obtained otoliths during a unique experiment conducted on juvenile sockeye salmon aged 1.0. Conditions of the experiment were designed to mimic the natural conditions that juvenile sockeye salmon experience in the first weeks of migration towards the open ocean. Juvenile sockeye salmon (from the Pitt River stock) were reared from fry to the smolt stage in tanks with fresh water at an ambient temperature of 9–11 °C and a natural light/dark cycle in the experimental facility operated by the Department of Fisheries and Oceans at the Pacific Biological Station, Nanaimo, BC, Canada. At age 1.0 (smoltification period), the fish were transferred into experimental tanks supplied with freshwater. After 2 days, the fish were transitioned to saltwater in two steps. On the first day, 50 % of freshwater was replaced with saltwater; on the second day (referred to as «Day 0» in this study), the water was replaced with 100 % saltwater (with a salinity of 28 psu). The fish were fed a ration of 1.5 % body weight (BW) day⁻¹ until Day 7. On Day 8, fish were transitioned to three different treatment rations, in triplicate, i.e., 3 tanks in each treatment: (1) 0.25 % BW day⁻¹ (food-deprived (FD) treatment), (2) 0.50 % BW day⁻¹, and (3) 1.50 % BW day⁻¹ (food-replete (CR) control treatment). After 14 days (Day 22), feeding levels were returned to 1.5 % BW day⁻¹ in all tanks for another 14-day period (to Day 36), by completion of which the experiment was terminated. Throughout the experiment, the fish were exposed to a natural seasonal photoperiod at a latitude 49° N and a constant ambient temperature (~10.5 °C). The saltwater was supplied from the Strait of Georgia after sand filtering and UV treatment. All the sampled fish were euthanized with a lethal dose of anaesthetic (MS222). The fork length and wet weight of the experimental fish were measured and sagittal otoliths extracted.

Otolith preparation. For this study, we used otoliths from the fish collected on Day 28 (Group A) and Day 35 (Group B) from the FD and CR groups. The sagittal otoliths from each fish were cleaned and washed in the Milli-Q water. The otoliths were then air-dried for at least 48 h, weighed, and photographed. Damaged or vaterite otoliths were discarded. Otolith width was measured at the widest point along the dorsal-ventral axis.

Each otolith was embedded in resin [Araldite 502, https://www.tedpella.com/chemical_html/chem2.htm#anchor18052], positioned sulcus side up, sectioned (transverse sections

with the inclusion of the core), and polished (with 30, 3, and 0.3 μm lapping film) from both sides until daily circuli were clearly visible. The polished otolith sections were mounted on microscopic slides, washed with Milli-Q water, and air-dried. Each otolith section was photographed at magnifications 25 \times , 110 \times , and 400 \times (Axio scope A1, Zeiss Universal; www.zeiss/microscopy) before and after laser ablation.

Microstructure examination. Previous studies on larval and juvenile stages of a variety of fish species have demonstrated a correlation between number of days and otolith increments at a ratio of 1 : 1 [Campana, Neilson, 1985; Freshwater et al., 2015]. Therefore, we assumed the daily formation of increments, which allowed us to identify the actual circulus that corresponded to the first day of the experiment (Day 1).

For each otolith, the number of daily increments (days) was counted back from the edge of the otolith to Day 1 of the experiment. A small number of otoliths ($n = 6$) were removed from analysis due to the low contrast of their daily circuli.

LA-ICPMS method. To determine the Sr-based sea entry mark, we used LA-ICP-MS. To increase the horizontal sampling resolution, a rectangular slit of $4 \times 50 \mu\text{m}$ was used for ablation of otoliths at a speed of $1 \mu\text{m} \cdot \text{s}^{-1}$ and repetition rate of 15Hz (see Tabl. 1 for additional parameters). This allowed for $4 \mu\text{m}$ resolution sampling, equivalent to 2–3 daily increments. Three isotopes were monitored in this study: ^{43}Ca , ^{44}Ca , and ^{86}Sr . Raw data obtained with the instrument were reduced using Iolite, a self-contained package for Igor Pro[®] (Wavemetrics Inc. of Lake Oswego, Oregon, USA) [Paton et al., 2011]. Trace element concentrations and ratios were determined by external calibration using the standard reference materials (SRM) of the National Institute of Science and Technology (NIST): synthetic silicate glass SRM NIST 612 and 610. Instrument drift was corrected for assuming $\text{Ca} = 40 \%$ as the internal standard for carbonates. The SRM NIST 610 and the USGS microanalytical carbonate standard MACS-3 were monitored for quality control purposes. Detection limits were below 5 ppm for Sr, and all sample concentrations were above detection limits (Tabl. 2).

Table 1
LA-ICP-MS settings, operating conditions and data acquisition parameters
for multi-element analysis of otolith samples

Table 1

Таблица 1
Настройки LA-ICPMS, условия работы и параметры сбора данных
для многоэлементного анализа проб отолитов

Laser ablation parameters	
Instrument model	Photon Machines Analyte G2
Wavelength, nm	193
Ablation gas	He
He flow rate, mL · min ⁻¹	800
Ablation mode	Scan line with rotating slit
Slit size, μm	4×50
Repetition rate, Hz	15
Scan rate, $\mu\text{m} \cdot \text{s}^{-1}$	1
Fluence, J · cm ⁻²	6.9
ICP-MS parameters	
Instrument model	Thermo Scientific X-Series II
RF power, W	1350
Carrier gas	Ar
Ar flow rate, L · min ⁻¹	0.60
Isotopes monitored	^{43}Ca , ^{44}Ca , ^{86}Sr
Standards	SRM NIST 612 and 610, MACS-3
Internal standard element	Ca

Mean Sr concentrations and relative standard deviations for multiple laser paths on NIST 612 and MACS3 are given in Tabl. 2. Relative standard deviation in Sr concentrations

Table 2

Strontium concentrations, limits of detection (LOD), and relative standard deviations (RSD) for SRM NIST 610, MACS-3, and otoliths samples. Note that NIST610 was used as a reference (so no LOD was calculated for this standard)

Таблица 2

Концентрации стронция, пределы обнаружения (LOD) и относительное стандартное отклонение (RSD) для стандартов NIST 610, MACS-3 и образцов отолигов

Standards and otoliths	Sr concentration (ppm) (\pm SE)	LOD (ppm) (\pm SE)	RSD
NIST 610	508 (29)	–	6.4
MACS-3	6776 (418)	5.7 (0.7)	7.7
Otoliths	1080 (223)	3.9 (1.0)	20.0

was 7.7 % for MACS-3 and 6.4 % for NIST 610. Average Sr concentrations in MACS-3 standards during our experiment were only by 2 % lower than in standard documentation and, thus, no adjustment was applied.

The breakpoint (the point at which the Sr : Ca ratio changed substantially) was determined based on the change in the Sr : Ca signal. Segmented regression analysis (SRA) was performed using the R statistical software ‘*segmented*’ [Stocks et al., 2014; Freshwater et al., 2015; <https://www.R-project.org/>].

First, we assumed that the point in time when Sr rapidly changes concentration is the point of saltwater entry [Stocks et al., 2014], as fish experience a rapid change in environmental concentrations of Sr and the incorporation is mainly driven by ambient concentrations [Walther, Thorrold, 2006]. In our analysis, we used only the area of the signal that included the last sharp increase in the Sr ratio and the prior segment. Below is the step-by-step protocol for determination of the Sr signal position relative to the true point of saltwater entry in otoliths.

Step 1. Otoliths were photographed, and the laser was run on the selected areas. We used a rectangular slit of $4 \times 50 \mu\text{m}$ to increase the breakpoint estimation accuracy [Stocks et al., 2014]. Daily increment counts were performed alongside the ablated area (Fig. 1). The actual point of transition to saltwater was identified (Day 1) by counting either 28 or 35 increments (Group A and B respectively) from the edge of the otolith.

Step 2. After determining the distance from the start of the laser path to the breakpoint, the distance from the otolith edge to the breakpoint was measured and marked in the post-ablation photographs.

Step 3. Daily increment counts were performed within the marked area (Fig. 1). First, the actual point of transition to saltwater was identified by counting either 28 or 35 increments (Group A and B, respectively) from the otolith edge.

Step 4. The Sr identified breakpoint was located along the same marked transect using the distance in Step 2.

Step 5. Finally, the difference in the number of increments (days) between the actual transition day and the day of Sr signal appearance was estimated.

All counts and measurements were performed in duplicates. The final number of the otoliths used in this analysis was 17.

To evaluate the relationship between the fish length/weight and the Sr signal time lag due to non-normal distribution we used Spearman’s rank correlation analysis. We used unpaired Welch’s *t*-tests to test for differences in signal lags between the FD and CR treatment groups [<https://www.R-project.org/>].

A Bayesian approach using the Markov Chain Monte Carlo (MCMC) simulation [Bhattacharya et al., 2016] was used to estimate population parameters of Sr signal delay, using non-informative normal distributions as priors. To perform MCMC estimation, we utilised jags within R [v3.4.3, <https://www.R-project.org/>], with the package R2jags [<http://CRAN.R-project.org/package=R2jags>].

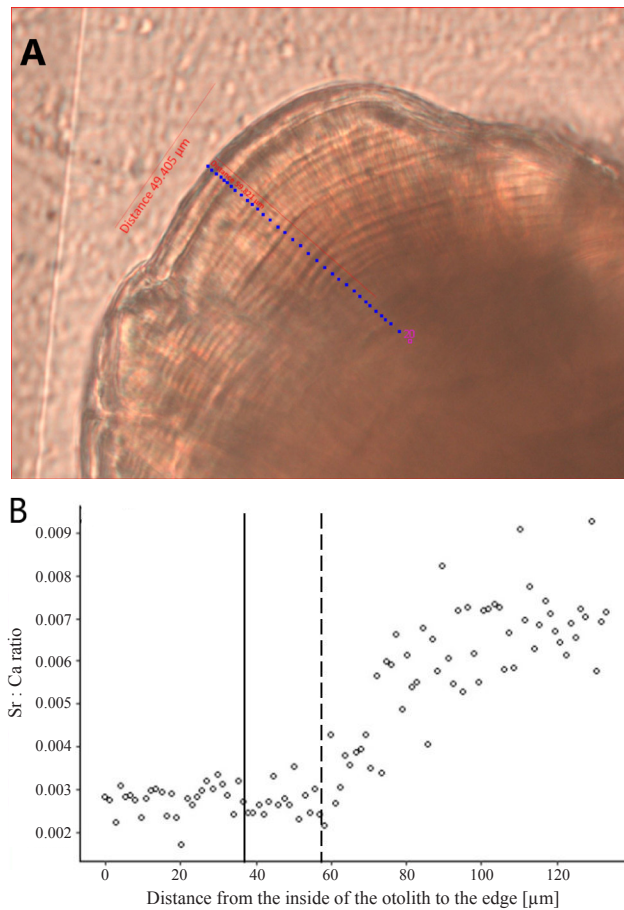


Fig. 1. Example of combination of microstructure and trace elements signals to determine the Sr signal breakpoint position: **A** — daily increments in the pre-ablation image (*blue dots*), with the position of ablation path and the distance from the edge of the otoliths to the estimated Sr signal breakpoint; **B** — breakpoint estimation outcome. Breakpoint indicated by the dashed line (X-axis is the distance from the laser start; Y-axis is the Sr : Ca ratio; vertical dashed line is the estimated breakpoint; vertical solid black line is the Day 1 increment position). For illustration, the fish with ID no. 252 (see Tabl. 3) had a 8-day delay, with a 20- μm difference between the Day 1 increment and the Sr : Ca ratio estimated breakpoint

Рис. 1. Пример комбинации сигналов микроструктуры и микроэлементов для определения положения точки излома сигнала Sr: **A** — ежедневные приращения на изображении до абляции (*синие точки*) с указанием положения пути абляции и расстояния от края отолитов до предполагаемой точки излома сигнала Sr; **B** — результат оценки точки останова. Точка останова указана пунктирной линией (расстояние по оси *x* от запуска лазера, отношение Sr : Ca по оси *y*, вертикальная пунктирная линия представляет собой расчетную точку останова, вертикальная сплошная черная линия представляет собой положение приращения в день 1). Например, у рыбы № 252 (табл. 3) задержка составила 8 дней, с разницей в 20 мкм между приростом в 1-й день и расчетной контрольной точкой отношения Sr : Ca

Discussion of results

The average fish body length and weight for Group A (Day 28) and B (Day 35) combined were 150 mm (with a range of 141–170 mm) and 37 g (24–57 g), respectively. The mean daily otolith growth increment width for Group A was 1.8 μm , with an average total otolith width of 45 μm from Day 1 to Day 28. For Group B, the mean daily otolith growth increment was 1.5 μm , with an average total otolith width of 62 μm from Day 1 to Day 35. Nine of the otoliths from our dataset were from fish of the food-deprived (FD) group (Tabl. 3). We did not

Table 3
Sr concentrations and lags in Sr signal and visual mark appearance relative to the actual first day in salt water estimated by counting daily increments

Таблица 3
Концентрации Sr, отставание в сигнале Sr и появление визуальной метки по сравнению с фактическим первым днем в соленой воде, оцененные путем подсчета суточных приращений

Fish ID	Time in salt water (weeks)	Treatment	Body weight (g)	Body length (mm)	Visual saltwater check mark delay (days)	Sr signal delay (days)	Sr (ppm) before salt water transition (min-max)	Sr (ppm) after salt water transition (min-max)
181	28 (A)	1.5	31.27	141	NA	2	768 (734–802)	1976 (1453–22780)
183	28 (A)	1.5	26.04	136	2	9	975 (895–1071)	3085 (3026–3203)
190	28 (A)	0.25	33.76	145	NA	0	810 (NA)	2403 (2060–2977)
192	28 (A)	0.25	32.15	143	NA	9	1678 (1543–1812)	2228 (1844–2609)
203	28 (A)	0.25	33.02	150	NA	5	745 (598–895)	865 (752–1052)
204	28 (A)	0.25	30.26	141	NA	11	1024 (815–1161)	1873 (1670–2212)
211	28 (A)	1.5	46.68	163	NA	5	1000 (905–1033)	2336 (2208–2450)
212	28 (A)	1.5	57.72	170	NA	9	1335 (1112–1614)	2449 (2081–2450)
218	35 (B)	1.5	40.52	153	NA	12	968 (853–1354)	2483 (2392–2897)
220	35 (B)	1.5	55.80	170	NA	22	1016 (907–1059)	2142 (1741–2348)
223	35 (B)	0.25	35.78	147	0	10	937 (849–1128)	2707 (2545–2941)
224	35 (B)	0.25	24.58	134	0	10	840 (643–1148)	2234 (1863–2791)
228	35 (B)	0.25	34.15	151	1	3	819 (700–858)	2561 (2191–3330)
236	35 (B)	0.25	41.82	155	NA	14	1690 (1478–1910)	3012 (2964–3315)
237	35 (B)	0.25	33.63	147	0	6	866 (819–1035)	2462 (2324–2659)
247	35 (B)	1.5	45.54	160	3	5	949 (861–1123)	2489 (2274–3231)
252	35 (B)	1.5	41.24	157	3	8	960 (769–1149)	2308 (2191–2429)

expect to see any difference in Sr lag between the FD and the food replete (CR) groups, as the change in water Sr concentrations occurred 7 days before the feeding experiment started. Although the FD fish demonstrated a slightly shorter Sr signal lag compared to the CR group (7.6 days (SD = 4.3) in FD vs. 9.0 days (SD = 6.1) in CR), it was not significantly different (*t*-test, *p* = 0.58) and justified pooling the data for further analysis.

In all 17 otoliths, the saltwater Sr signal appeared after the actual day (Day 1) of saltwater entry estimated by counting daily increments, with an average lag of 8.2 days (SD = 5.1) and 15 μm (Tabl. 3, Fig. 2), which was also confirmed by the MCMC simulation outcomes (Fig. 3) demonstrating that the pick of the population occurs at the 8-day delay. All saltwater Sr signals registered after the true day of saltwater transition (Fig. 3). This result is similar to that obtained by Miller [2011], who experimented with juvenile Chinook salmon of smaller fork length (average 55.8 mm). That experiment however demonstrated a shorter (2–4 days) delay in saltwater Sr signal appearance. In our experiment, the average initial size of juvenile sockeye was 2.5-fold larger (141 mm), and the signal delay was 2-fold longer. This suggests that the speed of the Sr signal appearance could negatively correlate with fish size as, was observed by Zimmerman [2005] for a group of salmonid species (juvenile Chinook salmon *O. tshawytscha*, coho salmon *O. kisutch*, sockeye salmon *O. nerka*, rainbow trout *O. mykiss*, and Arctic char *Salvelinus alpinus*). We, however, could not confirm this due to the narrow size range of the experimental fish.

Several previous studies identified the benefits of using a combination of microstructure analysis and chemical marks to evaluate habitat shifts. Freshwater et al. [2015] used experimental fish otoliths with the known day of marine entry to confirm that visual saltwa-

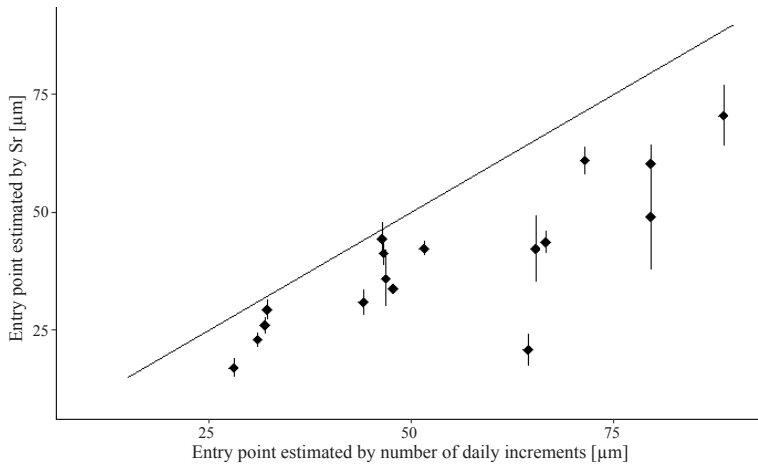


Fig. 2. Microstructural (daily increments) and chemical (Sr concentrations) estimates of salt water entry point. The distances on the X- and Y-axis are distances from the otolith edge (in μm) to Day 1 of the experiment (salt water entry). The chemical estimates have a 95 % confidence interval (C.I.) calculated using breakpoints in the regression of Sr concentrations across the otolith transect. The central line represents a 0 difference between two types of estimates. The points closest to the central line have a minimal difference between the chemical estimates and the microstructural estimates. All points are below this line, which indicates that chemical estimated points are in all cases further from the core and, thus, occurred later in the life history of fish.

Рис. 2. Микроструктурные (суточные приросты) и химические (концентрации Sr) оценки точки входа соленой воды. Расстояние по осям x и y — расстояние от края отолита (в $\mu\text{м}$) до 1-го дня эксперимента (вход соленой воды). Химические оценки имеют 95 % C.I., рассчитаны с использованием контрольных точек в регрессии концентраций Sr на разрезе отолитов. Центральная линия представляет нулевую разницу между двумя типами оценок. Ближайшие к центральной линии точки имеют минимальную разницу между химическими оценками и микроструктурными оценками. Все точки находятся ниже этой линии, что указывает на то, что химически оцененные точки во всех случаях находились дальше от сердцевины и, таким образом, возникали позже в жизненном цикле рыб

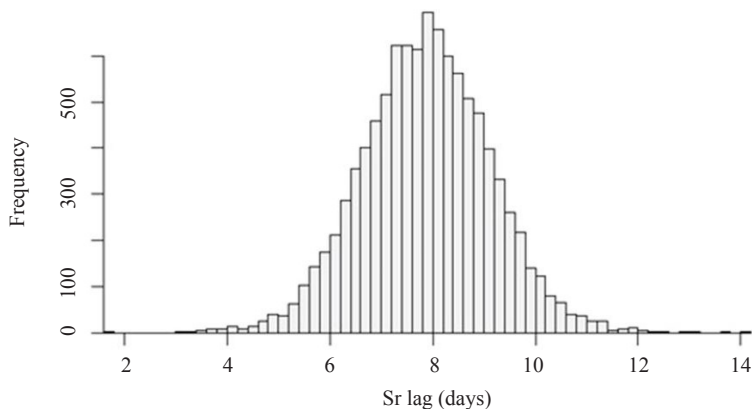


Fig. 3. *A posteriori* distribution of Sr lag (days)

Рис. 3. Апостериорное распределение задержки Sr

ter check marks appeared on the same day as the marine transition but did not validate the appearance of the Sr signal on the same set of otoliths. However, Freshwater et al. [2015] compared the appearance of the Sr signal shift and saltwater check mark in wild fish and found that the Sr signal occurred earlier, possibly due to some physiological processes. In our study, the visual sea entry mark was only visible in 7 out of 17 otoliths (presumably due to the artificial conditions of fish rearing). The presence of these marks in 7 otoliths allowed

us to compare the timing of appearance of the check mark and Sr breakpoint relative to the true day of entry estimated by the microstructural analysis. In 3 out of 7 otoliths, the check marks coincided in time with the saltwater entry day estimated by counting the number of increments, while in the remaining 4 otoliths, check marks appeared on days 1 to 3 after the increment estimated entry day (the true day). It is important that the visual saltwater check mark was not aligned with the Sr identified breakpoint, with the latter being delayed by 1 to 10 days relative to the visual saltwater check mark (Tabl. 3).

There may be methodological explanations for the discrepancy in the relative distance between the Sr estimated marine entry point in the otoliths and the actual transition point (estimated either by daily increments counts or visual saltwater check). First, the size of laser ablating spot influences the appearance of the signal due to horizontal mixing. For example, with a spot size of 15 μm , the Sr signal increase would appear by 15 μm earlier vs. the $4 \times 50 \mu\text{m}$ rectangular slit used in this study where the Sr signal appeared by 4 μm earlier than the actual point of Sr increase in otoliths.

Second, the section type used may also affect the timing of signal detection. The formation of circuli and the profile of sagittal sections (Fig. 4: top panel) indicate that during laser ablation vertical mixing of the signal from adjacent circulus may occur, i.e., where later formed circuli ablate together with the earlier circuli. This may cause the Sr signal shift to appear earlier than the visual marine transition mark. In the case of transverse sectioning used in our study, such mixing would be minimal (Fig. 4: bottom panel).

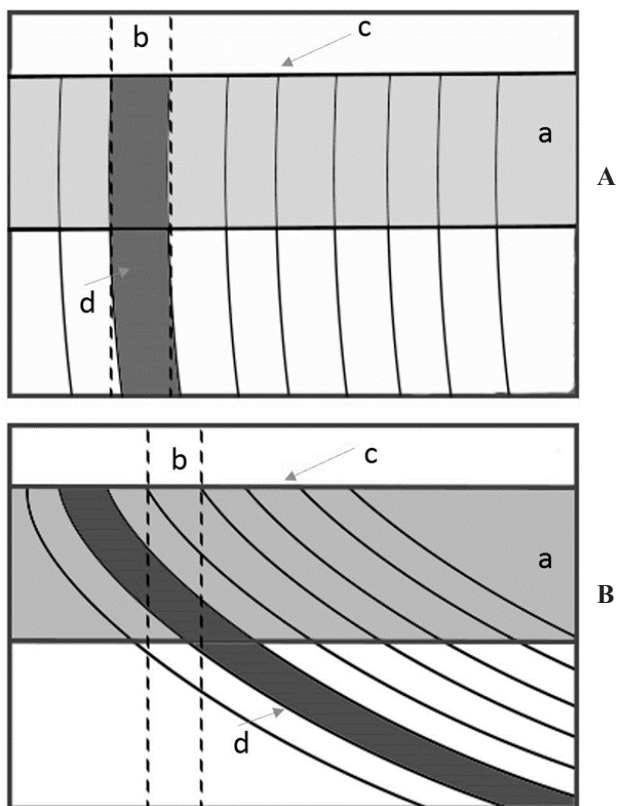


Fig. 4. Comparison of transverse and sagittal section profiles (the otolith core — edge direction is from right to left): **A** — transverse section profile; **B** — sagittal section profile; *a* — laser ablation depth; *b* — width of a daily increment; *c* — polished surface of the otolith; *d* — first increment with marine levels of Sr

Рис. 4. Сравнение профилей поперечного и сагиттального сечений (ядро отолида — ребро справа налево): **A** — изображение — профиль поперечного среза; **B** — профиль сагиттального сечения; *a* — глубина лазерной абляции; *b* — ширина суточного прироста; *c* — полированная поверхность отолида, *d* — первое приращение с морскими уровнями Sr

Conclusions

Our study provides high-resolution information (close to daily) on the behavior of Sr concentrations during the saltwater transition in otoliths of juvenile sockeye salmon (age 1.0). The Sr saltwater entry signal occurred, on average, by 8 days later than the actual day of fish transition to saltwater, with 95 % confidence interval between days 3 and 13. These values may be used to correct the marine entry timing estimations when using microchemistry. However, the time lag could be species-specific and size-dependent, which suggests the necessity of further experimental work to uncover the dynamics of the elemental signal in different size groups of sockeye salmon and other salmonid species. Transverse sectioning might be a preferable method for using a combination of microstructural and chemical markers due to the low to no mixing of signals from different layers of increments in this type of section.

Limitations

Due to the high sensitivity of the trace element analysis to contamination, it was impossible to use additional methods to obtain or validate daily growth patterns (staining and electron microscopy), which led to the elimination of a number of otoliths with low contrast circuli from the analysis. Furthermore, the analysis could be improved from the use of chemical marking of otoliths at the first day of the experiment as it would greatly increase the number of otoliths suitable for the analysis.

Acknowledgments

This research was funded by Four Year Doctoral Fellowship (UBC), NSERC Discovery grant and by the Aquaculture Collaborative Research and Development Program (ACRDP) in partnership with the BC Salmon Farmers Association. Julia C. Bradshaw set up and ran the feeding trial and aquarium services staff at PBS looked after the fish.

Ethics statement

All work with animals was performed in a strict accordance with the recommendations set out in the Canadian Council on Animal Care (CCAC) Guide to the Care and Use of Experimental Animals. The protocols were approved by the Pacific Region Animal Care Committee (Animal Use Protocol No.: 14-008). Fish were euthanized by a lethal dose of the MS222 anaesthetic.

References

- Bath, G.E., Thorrold, S.R., Jones, C.M., Campana, S.E., McLaren, J.W., and Lam, J.W.H.**, Strontium and barium uptake in aragonitic otoliths of marine fish, *Geochim. Cosmochim. Acta*, 2000, vol. 64, pp. 1705–1714. doi 10.1016/S0016-7037(99)00419-6
- Beamish, R.J., Mahnken, C., and Neville, C.M.**, Evidence That Reduced Early Marine Growth is Associated with Lower Marine Survival of Coho Salmon, *Trans. Am. Fish. Soc.*, 2004, vol. 133, pp. 26–33.
- Bhattacharya, R., Lin, L., and Patrangenu, V.**, *A Course in Mathematical Statistics and Large Sample Theory*, New York: Springer, 2016.
- Campana, S.E.**, Chemistry and composition of fish otoliths: Pathways, mechanisms and applications, *Mar. Ecol. Prog. Ser.*, 1999, vol. 188, pp. 263–297. doi 10.3354/MRPS188263
- Campana, S.E., Chouinard, G.A., Hanson, J.M., Fréchet, A., and Bratney, J.**, Otolith elemental fingerprints as biological tracers of fish stocks, *Fish. Res.*, 2000, vol. 46, Iss. 1–3, pp. 343–357. doi 10.1016/S0165-7836(00)00158-2
- Campana, S.E. and Neilson, J.D.**, Microstructure of Fish Otoliths, *Can. J. Fish. Aquat. Sci.*, 1985, vol. 42, no. 5, pp. 1014–1032. doi 10.1139/f85-127
- Campana, S.E. and Thorrold, S.R.**, Otoliths, increments, and elements: keys to a comprehensive understanding of fish populations?, *Can. J. Fish. Aquat. Sci.*, 2001, vol. 58, no. 1, pp. 30–38. doi 10.1139/f00-177

Eldson, T.S., Wells, B.K., Campana, S.E., and Gillanders, B.M., Otolith chemistry to describe movements and life-history parameters of fishes: Hypotheses, assumptions, limitations and inferences, *Oceanogr. Mar. Biol.*, 2008, vol. 46, pp. 297–330.

Freshwater, C., Trudel, M., Beacham, T.D., Neville, C.E., Tucker, S., and Juanes, F., Validation of daily increments and a marine-entry check in the otoliths of sockeye salmon *Oncorhynchus nerka* post-smolts, *J. Fish Biol.*, 2015, vol. 87, pp. 169–178. doi 10.1111/jfb.12688

Henderson, M.A. and Cass, A.J., Effect of Smolt Size on Smolt-to-Adult Survival for Chilko Lake Sockeye Salmon (*Oncorhynchus nerka*), *Can. J. Fish. Aquat. Sci.*, 1991, vol. 48, no. 6, pp. 988–994. doi 10.1139/f91-115

Irvine, J.R. and Akenhead, S.A., Understanding Smolt Survival Trends in Sockeye Salmon, *Marine and Coastal Fisheries: Dynamics, Management, and Ecosystem Science*, 2013, vol. 5, Iss. 1, pp. 303–328. doi 10.1080/19425120.2013.831002

Kerr, L.A. and Campana, S.E., Chemical Composition of Fish Hard Parts as a Natural Marker of Fish Stocks, *Stock Identification Methods*, 2014, pp. 205–234. doi 10.1016/B978-0-12-397003-9.00011-4

Koenings, J.P., Geiger, H.J., and Hasbrouck, J.J., Smolt-to-Adult Survival Patterns of Sockeye Salmon (*Oncorhynchus nerka*): Effects of Smolt Length and Geographic Latitude when Entering the Sea, *Can. J. Fish. Aquat. Sci.*, 1993, vol. 50, pp. 600–611.

Miller, J.A., Effects of water temperature and barium concentration on otolith composition along a salinity gradient: Implications for migratory reconstructions, *J. Exp. Mar. Biol. Ecol.*, 2011, vol. 405, no. 1, pp. 42–52. doi 10.1016/j.jembe.2011.05.017

Nelson, T.R. and Powers, S.P., Validation of species specific otolith chemistry and salinity relationships, *Environ. Biol. Fish.*, 2019, vol. 102, no. 5, pp. 801–815. doi 10.1007/s10641-019-00872-9

Paton, C., Hellstrom, J., Bence P., Woodhead, J., and Hergt, J., Iolite: freeware for the visualisation and processing of mass spectrometric data, *J. Anal. At. Spectrom.*, 2011, vol. 26, Iss. 12, pp. 2508–2518.

Team, R.C., R: A language and environment for statistical computing. R Foundation for Statistical Computing, Vienna, Austria, 2021, URL: <https://www.R-project.org/>.

Stocks, A.P., Pakhomov, E.A., and Hunt, B.P.V., A simple method to assess the marine environment residence duration of juvenile sockeye salmon (*Oncorhynchus nerka*) using laser ablation, *Can. J. Fish. Aquat. Sci.*, vol. 71, no. 10, pp. 1437–1446. doi 10.1139/cjfas-2014-0073

De Villiers, S., Nelson, B.K., and Chivas, A.R., Biological Controls on Coral Sr/Ca and $\delta^{18}\text{O}$ Reconstructions of Sea Surface Temperatures, *Science*, 1995, vol. 269, no. 5228, pp. 1247–1249. doi 10.1126/science.269.5228.1247

Walther, B.D. and Limburg, K.E., The use of otolith chemistry to characterize diadromous migrations, *J. Fish Biol.*, 2012, vol. 81, no. 2, pp. 796–825. doi 10.1111/j.1095-8649.2012.03371.x

Walther, B.D. and Thorrold, S.R., Water, not food, contributes the majority of strontium and barium deposited in the otoliths of a marine fish, *Mar. Ecol. Prog. Ser.*, 2006, vol. 311, pp. 125–130. doi 10.3354/meps311125

Welch, D.W., Porter, A.D., Rechisky, E.L., Challenger, W.C., and Hinch, S.G., Critical periods in the marine life history of Pacific Salmon?, *NPAFC. Tech. Rep.*, 2013, no. 9, pp. 179–183.

Yokouchi, K., Fukuda, N., Shirai, K., Aoyama, J., Daverat, F., and Tsukamoto, K., Time lag of the response on the otolith strontium/calcium ratios of the Japanese eel, *Anguilla japonica* to changes in strontium/calcium ratios of ambient water, *Environ. Biol. Fish.*, 2011, vol. 92, pp. 469–478. doi 10.1007/s10641-011-9864-5

Zhang, Z. and Beamish, R.J., Use of otolith microstructure to study life history of juvenile chinook salmon in the Strait of Georgia in 1995 and 1996, *Fish. Res.*, 2000, vol. 46, pp. 239–250. doi 10.1016/S0165-7836(00)00149-1

*The article was submitted 7.02.2022; approved after reviewing 30.03.2022;
accepted for publication 20.05.2022*

Поступила в редакцию 7.02.2022 г.

После доработки 30.03.2022 г.

Принята к публикации 20.05.2022 г.